JOURNAL OF CATALYSIS 124, 41–51 (1990)

Preparation and Characterization of $LaMn_{1-x}Cu_xO_{3+\lambda}$ Perovskite Oxides

M. L. ROJAS,* J. L. G. FIERRO,*,[1] L. G. TEJUCA,*,[2] AND ALEXIS T. BELL†

*Instituto de Catálisis y Petroleoquímica, CSIC, Serrano, 119, 28006 Madrid, Spain; and †Department of Chemical Engineering, University of California, Berkeley, California 94720-9989

Received September 26, 1989; revised January 18, 1990

Compounds of nominal composition $LaMn_{1-x}Cu_xO_{3+\lambda}$ ($0 \leq x \leq 1$) have been prepared and characterized by means of X-ray diffraction, X-ray photoelectron spectroscopy (XPS), and temperature-programmed reduction (TPR). Substitution of manganese by copper up to $x = 0.6$ preserves the perovskite structure. For $x = 0.8$, in addition to the perovskite, La_2CuO_4 and CuO were formed. For $x = 1$, the only phases present were La_2CuO_4 and CuO. The perovskites showed oxidative nonstoichiometry for $x \leq 0.4$ and reductive nonstoichiometry for $x = 0.6$. Stoichiometry was reached for $x = 0.5$. XPS results for $LaMn_{0.6}Cu_{0.4}O_{3+\lambda}$ reduced at 473–753 K are indicative of sintering of the copper particles when reduction is effected above 673 K. The TPR curve for $LaMnO_{3+\lambda}$ showed an inflection point at ca. 0.5 e^- per molecule which nearly corresponds to reduction of the estimated oxygen excess in the sample. Samples with substitutions $0 \leq x \leq 0.6$ showed two reduction steps of Cu^{2+} to Cu^0 and of Mn^{n+} ($n \geq 3$) to Mn^{2+}. In the fully substituted sample ($x = 1$) reduction of CuO and reduction of La_2CuO_4 can be clearly distinguished. Reduction of perovskites of low copper content ($x < 0.5$) at 673 K or below yielded highly dispersed copper catalysts.

INTRODUCTION

$LaMnO_{3+\lambda}$ and $LaMnO_{3+\lambda}$-based perovskites have been found to exhibit a wide range of oxidative (excess of oxygen) and reductive (oxygen deficiency) nonstoichiometry (*1–11*). This is a most important property for study since the departure from stoichiometry affects substantially the physical and chemical properties of these compounds. The degree of nonstoichiometry depends on the preparation variables, mainly the oxygen partial pressure of the surrounding atmosphere and the final calcination temperature, so that higher P_{O_2} and lower calcination temperatures tend to increase λ in $LaMnO_{3+\lambda}$ (*1–3, 5*). An alternative method of varying the oxygen content in $LaMnO_{3+\lambda}$ is by partial substitution of the metal cations with cations of a valence lower than 3+, leading to multicomponent perovskites. Substitution in position B has a profound effect on the catalytic performance of these materials because of the presence of two active metal cations. By contrast, partial substitution of the A cation has a less important and a less known effect on their surface and catalytic properties (*12*).

Perovskite oxides have been used for the synthesis of oxygenated products (mainly alcohols) from CO + H_2 by a number of authors (*13–17*). Broussard and Wade (*16*) reported that no oxygenated products are formed using $LaMnO_{3+\lambda}$ as catalyst. However, the partially substituted $LaMn_{0.5}Cu_{0.5}O_3$ oxide exhibited high methanol selectivity. These results suggest that copper is the catalytic agent for this reaction. From data obtained with other perovskite systems these authors concluded that the catalytic sites are higher valence (>0) surface cations in position B. Likewise, Monnier and Apai (*15*), using promoted Cu–Cr oxide catalysts for CO hydrogenation, reached the conclusion that Cu^+ is required for CO chemisorption while metallic Cu^0 is re-

[1] To whom correspondence should be addressed.
[2] Deceased.

0021-9517/90 $3.00

quired for hydrogen chemisorption and subsequent reduction to form CH_3OH. In agreement with these findings Somorjai *et al.* (*13, 14*) reported that the active catalyst for CO hydrogenation over $LaRhO_3$ contained Rh^+ and Rh^0. It appears, therefore, that oxidized states of copper should play an important role as catalytic agents in the formation of oxygenates from synthesis gas over copper perovskites. However, the studies carried out so far, mostly of an empirical character, give little information on the properties of the solid catalysts.

In this laboratory, the series of La $Mn_{1-x}Cu_xO_{3+\lambda}$ oxides will be used for CO and CO_2 hydrogenation. In this work, some bulk and surface properties of these perovskites were studied by means of X-ray diffraction, XPS, and temperature-programmed reduction. Their catalytic activity for CO oxidation and their oxygen nonstoichiometry have been studied by Gallagher *et al.* (*18*) and Vogel *et al.* (*6*). The CO oxidation of La_2CuO_4, with the perovskite-related structure of K_2NiF_4, has been studied by Gunasekaran *et al.* (*19*).

EXPERIMENTAL

Materials. The $LaMn_{1-x}Cu_xO_{3+\lambda}$ catalysts were prepared by amorphous citrate decomposition as described previously (*20*). The decomposition of precursors has been effected by heating in air at 973 K for 5 h. BET specific surface areas of the samples as determined by N_2 adsorption at 77 K are given in Table 1. In the synthesis, $La(NO_3)_3 \cdot 6H_2O$, $Mn(NO_3)_2 \cdot 4H_2O$, and citric acid monohydrate (p.a. from Merck), and $Cu(CH_3COO)_2 \cdot H_2O$ reagent (pure from Carlo Erba) were used. Other compounds used in temperature-programmed reduction and XPS were MnO_2 prepared by thermal decomposition of $Mn(NO_3)_2 \cdot 4H_2O$ (p.a. from Merck); Mn_2O_3 (p.a. from Merck); CuO analytical reagent (from Mallinckrodt); and La_2O_3, obtained by thermal decomposition of $La(NO_3)_3 \cdot 6H_2O$ (p.a. from Merck). The gases used were high purity He(99.998%) and H_2(99.99%).

TABLE 1

BET Specific Surface Area[a] of Samples with Nominal Composition $LaMn_{1-x}Cu_xO_{3+\lambda}$

x	Specific surface area ($m^2\ g^{-1}$)
0	11.0
0.2	17.1
0.4	24.5
0.5	17.7
0.6	21.4
0.8	14.0
1.0	6.6

[a] From N_2 adsorption at 77 K. $S_{N_2} = 0.162$ nm^2.

Equipment and methods. X-ray photoelectron spectra were obtained with a Leybold–Heraeus LHS-10 spectrometer equipped with a magnesium anode (Mg$K\alpha$ = 1253.6 eV) operated at 12 kV and 10 mA and a data acquisition system for accumulation and storage of spectra. The powder under analysis was pressed in a small Inox cylinder with a 1-mm-deep hole. Spectra were recorded for outgassed(a) and reduced(b) samples. (a) The sample was outgassed in a high vacuum at 723 K for 2 h and then contacted with helium at atmospheric pressure to avoid exposure to air during its transfer to the spectrometer. (b) Sample reduction was effected by heating the as-prepared pressed powder at the desired temperature in a flow of 90 cm^3 min^{-1} He. Then a flow of 90 cm^3 min^{-1} H_2 was passed through the reactor for 2 h. After that the temperature was lowered to 298 K in a flow of helium (as above) and the sample was transferred to the spectrometer following the same procedure used for the outgassed sample. The outgassed or reduced sample was then outgassed in the primary vacuum chamber at 10^{-5} Torr (1 Torr = 133.3 N m^{-2}) for 0.5 h and then introduced into the ultrahigh vacuum chamber and outgassed at 7×10^{-9} Torr for 0.5 h. C 1*s*, O 1*s*, Cu 2*p*, Mn 2*p*, and La 4*d* emissions were recorded for each sample. The C 1*s* line at

284.6 eV was taken as reference for measurement of the binding energies (BEs) of core level electrons.

Temperature-programmed reduction experiments were performed with a Cahn 2100 RG microbalance (operating at an accuracy of 10^{-5} g) connected to a gas-handling system. The 20-mg sample was first outgassed by passing a flow of 90 cm^3 min^{-1} He for 1 h at 673 K and then it was cooled to 373 K maintaining the helium flow; after this, the temperature was linearly increased at 4 K min^{-1} with a Stanton Redcroft Eurotherm programmer passing through the sample a H_2 flow (as above). The observed weight loss was taken as a measure of the reduction degree in terms of electrons (e^-) per molecule ($1e^-$ per molecule would amount to reduction of Mn^{3+} to Mn^{2+} or Cu^{2+} to Cu^{1+}). X-ray diffractograms were obtained with a Philips PW1716/30 diffractometer using Cu$K\alpha$ radiation and a Ni filter.

RESULTS AND DISCUSSION

X-ray Diffraction of Oxidized Samples

X-ray diffraction patterns were obtained of as-prepared samples with nominal composition $LaMn_{1-x}Cu_xO_{3+\lambda}$ ($0 \lesssim x \lesssim 1$). Representative diffractograms are given in Fig. 1. Substitution of manganese by copper up to $x = 0.6$ preserves the perovskite structure. This result is to be expected since the ionic radii of Mn^{3+} (0.66 Å, 1 Å = 10^{-1} nm) and Cu^{2+} (0.69 Å) are very similar. For $x = 0.8$, lines which can be indexed to orthorhombic $LaMn_{1-x}Cu_xO_{3+\lambda}$, orthorhombic La_2CuO_4, and monoclinic CuO appear. For total substitution of manganese ($x = 1$) the only phases present are La_2CuO_4 and CuO. Although the synthesis of $LaCuO_3$ has been reported by Demazeau *et al.* (*21*), this perovskite appears not to be stable under our experimental conditions. Gallagher *et al.* (*18*) and Vogel *et al.* (*6*) have reported formation of the perovskite together with La_2CuO_4 and CuO for high substitutions of manganese by copper ($0.7 \lesssim x \lesssim 1$) in $LaMnO_{3+\lambda}$.

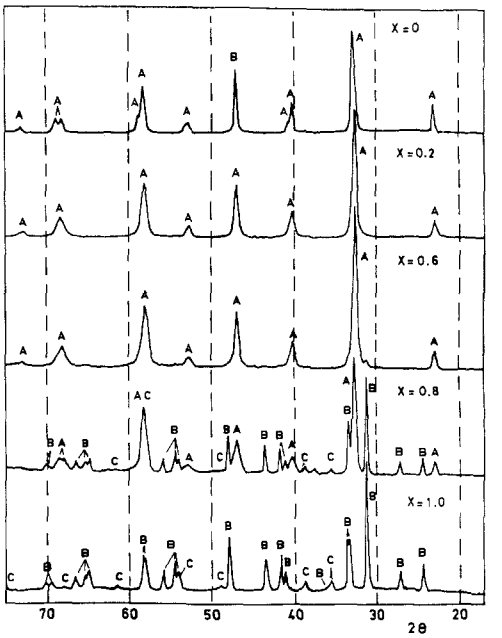

FIG. 1. X-ray diffraction patterns (Cu$K\alpha$ radiation) of samples with nominal composition $LaMn_{1-x}Cu_xO_{3+\lambda}$. (A) Orthorhombic $LaMn_{1-x}Cu_xO_{3+\lambda}$, (B) orthorhombic La_2CuO_4, (C) monoclinic CuO.

The end member of the series of $LaMn_{1-x}Cu_xO_{3+\lambda}$ oxides ($x = 1$) would have the formula $LaCuO_{2.5}$ (or $La_2Cu_2O_5$). This oxide has a tolerance factor, as defined by Goldschmidt, $t = r_A + r_O/\sqrt{2}(r_B + r_O)$ (r_A, r_B, and r_O being ionic radii in ABO_3) (*22, 23*) of 0.86, which explains its high instability. Compounds with the stoichiometry $A_2B_2O_5$ are known for a variety of A and B cations (*24, 25*). They are the first members ($n = 2$) of the $A_nB_nO_{3n-1}$ series of oxides (*26*) and are usually formed by reduction at low temperatures of the stoichiometric compound ABO_3. Thus, Crespin *et al.* (*27*) showed evidence of formation of $La_2Ni_2O_5$ by isothermal reduction in H_2 of $LaNiO_3$ at 585 K. However, at high temperatures (1273 K in He), this oxygen-deficient compound is not stable and, through a disproportionation reaction, is transformed in La_2NiO_4 and NiO according to the general equation

$$A_2B_2O_5 \rightarrow A_2BO_4 + BO. \qquad (1)$$

In agreement with these findings, Fierro *et al.* (*28*) identified these products after heating in He at 1073 K $LaNiO_3$ previously reduced in H_2 to ca. 1 e^- per molecule (i.e., B^{3+} reduced to B^{2+}) at 513 K. Formation of La_2CoO_4 and La_2NiO_4 has also been observed by Nakamura *et al.* (*8*) after heating $LaCoO_3$ and $LaNiO_3$ at 1273 K in a reducing atmosphere.

$LaMnO_{3+\lambda}$ exhibits oxidative nonstoichiometry (excess oxygen) (*5*). Substitution of Mn^{3+} by Cu^{2+} leads to a loss of oxygen and to the eventual appearance of oxygen vacancies as charge compensators. With increasing copper content, the concentration of oxygen vacancies increases and, for $x > 0.6$, becomes so high that the perovskite structure is no longer stable at the temperature used for sample preparation (973 K). $La_2Cu_2O_5$ is also unstable under these conditions. This would explain the partial disappearance of the perovskite structure for $x = 0.8$, and the complete disappearance of this structure for $x = 1$. The appearance of La_2CuO_4 and CuO as the principal structures observed for $x > 0.6$ is very likely due to a transformation similar to that expressed by Eq. (1).

The series of compounds with general formula $A_{n+1}B_nO_{3n+1}$ or $AO \cdot (ABO_3)_n$ contains perovskite sheets n units thick separated by one AO sheet with rock salt structure (*29, 30*). The structure of the first member of the series, A_2BO_4 ($n = 1$), and that of the perovskite ABO_3 are depicted in Fig. 2. It is seen that La_2CuO_4 can be regarded as closely related to the perovskite since the B atoms have the same environment of six oxygens arranged octahedrically in both cases. However, the A atoms in La_2CuO_4 are coordinated to nine oxygen atoms instead of the 12-coordination found in the perovskite. Therefore, the differences which may be observed in the catalytic behavior of the members of the oxide series with nominal composition $LaMn_{1-x}Cu_xO_{3+\lambda}$ should be derived (a) from their variable concentration in anion vacancies, (b) from the possible influence of the modifying A cation (differently coordinated in $LaMn_{1-x}Cu_xO_{3+\lambda}$ and La_2CuO_4) upon the catalytic active B cation, and (c) from the presence of CuO for a copper substitution $x > 0.8$. It should also be noted that the limiting composition A_2BO_4 of the above series allows the study of B^{2+} cations in oxides with a smaller B–O–B separation (and therefore with a stronger interaction) than is found in BO oxides with NaCl structure (*29*).

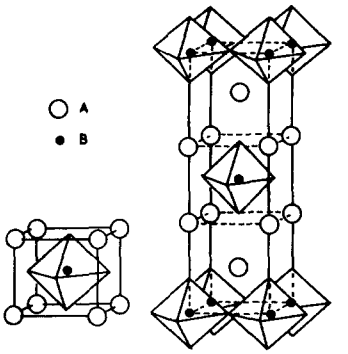

FIG. 2. Comparison of ABO_3 (left) and A_2BO_4 (right) structures. Oxygen atoms are situated at the vertexes of octahedra. Reproduced, by permission of the publisher, from Ref. (*29*).

XPS Results

The surface of the perovskite $LaMn_{0.6}Cu_{0.4}O_{3+\lambda}$ was studied by XPS. Mn 2*p*, Cu 2*p*, O 1*s*, and La 4*d* spectra were recorded for the outgassed sample in a high vacuum and for reduced samples in H_2 at 473–753 K. Spectra for Cu 2*p* are shown in Fig. 3. Selected BE values for these series of spectra are collected in Table 2. For comparison, the BEs of some reference compounds such as Mn_2O_3, CuO, and La_2O_3 are also included. The BE values for Mn 2*p* electrons in the outgassed and reduced perovskite practically coincide with those of Mn_2O_3. From these data it is not possible to distinguish whether one (Mn^{2+}) or two (Mn^{3+} and Mn^{2+}) ionic species are present on the surface since both Mn^{3+} and Mn^{2+} have essentially the same BE. The TPR results (Fig. 5d) would indicate, though, that the bulk Mn^{3+} remains unreduced after

TABLE 2

Binding Energies (eV) of Electrons of Different Atomic Levels in $LaMn_{0.6}Cu_{0.4}O_{3+\lambda}$ after Different Pretreatments and in Mn_2O_3, CuO, and La_2O_3 Reference Compounds

Compound	Pretreatment	Mn 2*p*		Cu 2*p*		O 1*s*		La 4*d*	
		1/2	3/2	1/2	3/2			3/2	5/2
$LaMn_{0.6}Cu_{0.4}O_{3+\lambda}$	High vacuum, 723 K	653.8	641.4	952.2	931.9	531.7	530.3	104.8	101.7
$LaMn_{0.6}Cu_{0.4}O_{3+\lambda}$	H_2, 473 K	653.9	641.3	952.3	932.0	531.4	530.4	105.3	102.0
$LaMn_{0.6}Cu_{0.4}O_{3+\lambda}$	H_2, 753 K	653.7	641.3	952.4	932.0	531.5	530.4	104.8	101.8
Mn_2O_3	As received	653.3	641.4	—				—	
CuO	As received	—		953.9	933.6	531.5	529.5	—	
La_2O_3	As received	—		—		532.6		105.8	102.7

reduction at 753 K. The BEs of Cu 2*p* electrons found after the different treatments are very similar. However, the Cu 2*p* spectra of the outgassed and reduced samples showed important differences with respect to the spectrum of CuO (Fig. 3). Thus, the BE of Cu $2p_{3/2}$ in CuO is situated ca. 1.7 eV upscale with respect to the corresponding BEs of the perovskite samples (Table 2). Also, CuO presents shake-up satellite peaks upscale from the main Cu 2*p* peaks. These satellites which are characteristic of Cu^{2+} ions are absent in the perovskite samples, indicating that the outgassing and reduction pretreatments yielded reduced copper species, presumably Cu^0, since this sample showed a bulk reduction of ca. 1.5 e^- per molecule at 723 K (Fig. 5d).

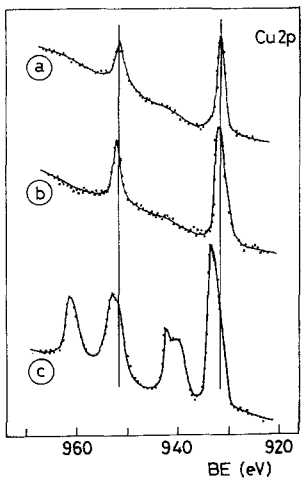

FIG. 3. Cu 2*p* spectra. (a) $LaMn_{0.6}Cu_{0.4}O_{3+\lambda}$ outgassed in a high vacuum at 723 K; (b) $LaMn_{0.6}Cu_{0.4}O_{3+\lambda}$ reduced in 90 cm^3 min^{-1} H_2 at 753 K; (c) CuO, as received.

O 1*s* spectra showed two peaks, at 530.3–530.4 eV of lattice oxygen O^{2-} and at 531.4–531.7 eV of hydroxyl species (*31–34*). The relative intensity of the peak at higher BE decreases slightly with increasing reduction temperature. These results are consistent with formation of a surface lanthanum hydroxide in the outgassed sample (not detected by X-ray diffraction) and its gradual decomposition after reduction into La_2O_3 and H_2O. The presence of hydroxyl groups in the outgassed sample is also supported by the observed broadening of the La $4d_{3/2}$ peak toward higher BEs, which indicates a decrease in the negative charge around the La^{3+} ion. Note that the reference La_2O_3 is highly hydroxylated since only one O 1*s* peak at 532.6 eV of OH^- groups was observed (Table 2). This most intense peak completely overlaps and masks the peak of lattice oxygen at lower BE. In this hydroxylated sample, the La $4d_{3/2}$ peak at 105.8 eV is situated at ca. 1 eV upscale with respect to the corresponding peak of the outgassed sample of the perovskite.

In Fig. 4 the O/(Cu + Mn) and Cu/Mn ratios calculated from the XPS spectra are represented as a function of the reduction

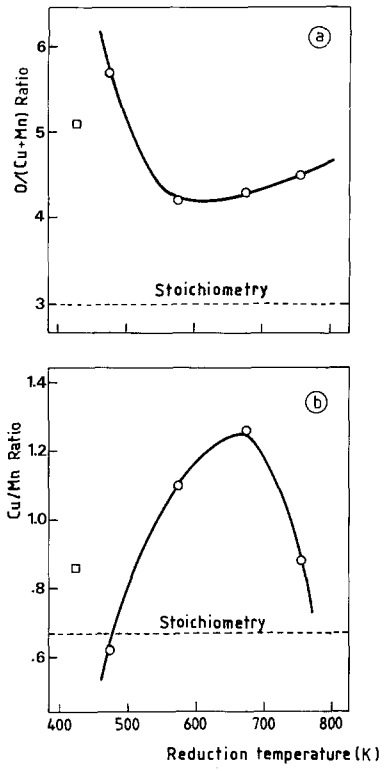

FIG. 4. Surface composition of $LaMn_{0.6}Cu_{0.4}O_{3+\lambda}$ after reduction in 90 cm^3 min^{-1} H_2 at increasing temperatures.

temperature. It is observed that the O/(Cu + Mn) ratio in the sample reduced at 473 K is twice that expected for the stoichiometric perovskite and undergoes a marked decrease in the samples reduced at 573 K and higher temperatures (Fig. 4a). This evolution is consistent with the presence of hydroxyl groups on the outgassed perovskite and their removal upon reduction. The Cu/Mn ratio of the sample reduced at 473 K (Fig. 4b) almost coincides with that expected for the stoichiometric perovskite. However, it increases remarkably for the sample reduced at 573 and 673 K and decreases for a reduction temperature of 753 K. These results are indicative of Cu^{2+} diffusion from bulk to surface upon reduction. Furthermore, the reduction at 753 K causes sintering of the copper particles on the surface. This finding emphasizes the importance of reducing perovskite at low temperatures to obtain a catalyst with a high copper dispersion.

Temperature-Programmed Reduction

TPR diagrams of the manganese and copper samples described above and of MnO_2 and CuO are shown in Figs. 5 and 6. Those corresponding to samples where a single perovskite phase is present ($0 \leq x \leq 6$) are represented in e^- per molecule vs reduction temperature. In samples where more than one phase has been detected ($0.8 \leq x \leq 1$), the reduction degree has been given as percentage weight loss. It is observed that MnO_2 is reduced to MnO at 673 K (Fig. 5a) and CuO to metallic Cu^0 at 473 K (Fig. 6d). Reduction of Mn^{3+} and Cu^{2+} in $LaMn_{1-x}Cu_xO_{3+\lambda}$ oxides is reached at substantially higher temperatures, showing the increased stability of these transition metal cations in the perovskite structure. In concurrence with these results, Wachowski *et al.* (*35*) have shown that $LaMO_3$ (M = Fe, Co, Ni) samples are more stable in a H_2 atmosphere than the respective simple oxides Fe_2O_3, Co_3O_4, and NiO. Reduction of the unsubstituted compound $LaMnO_{3+\lambda}$ (Fig. 5b) starts at ca. 500 K and reaches a constant weight, corresponding to a reduction of 1.48 e^- per molecule, at ca. 970 K. These temperatures are lower than those found previously for

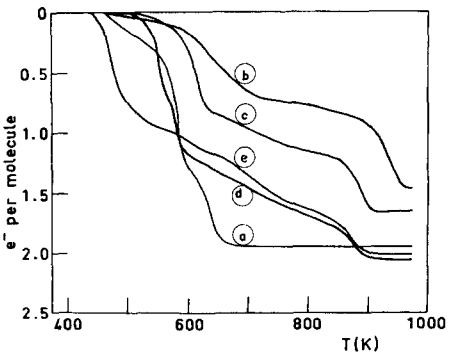

FIG. 5. Temperature-programmed reduction diagrams of MnO_2 (a) and $LaMn_{1-x}Cu_xO_{3+\lambda}$ (b, $x = 0$; c, $x = 0.2$; d, $x = 0.4$; e, $x = 0.5$) samples in a flow of 90 cm^3 min^{-1} H_2. Temperature ramp, 4 K min^{-1}.

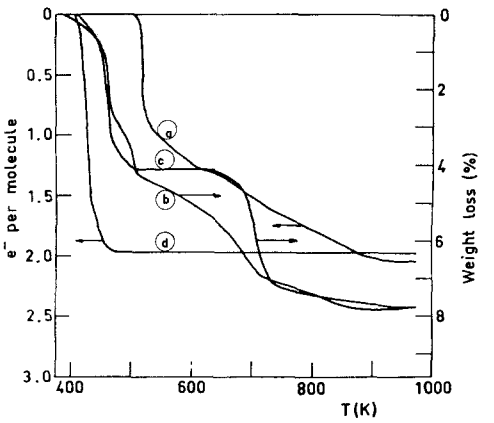

FIG. 6. Temperature-programmed reduction diagrams of samples with nominal composition $LaMn_{1-x}Cu_xO_{3+\lambda}$ (a, $x = 0.6$; b, $x = 0.8$; c, $x = 1.0$) and of CuO (d). Experimental conditions as in Fig. 5. Sample analysis in Fig. 1.

reduction of this perovskite under static conditions (300 Torr H_2) (*36*). The reduction curve shows an inflection point at ca. 0.5 e^- per molecule which nearly corresponds to reduction of the estimated excess of oxygen in the sample (see below). A similar effect has been observed in the reduction of $LaMnO_{3.13}$ (*6*) and $LaFeO_{3.18}$ (*37*). However, in the copper-substituted samples exhibiting oxidative nonstoichiometry ($x = 0.2$ and $x = 0.4$, see below), reduction of the excess oxygen cannot be distinguished from reduction of the stoichiometric oxygen (Figs. 5c and 5d).

In the TPR curves for $0 \leq x \leq 0.6$ two different reduction steps can be seen, the first associated with reduction of Cu^{2+} to Cu^0 and the second with reduction of Mn^{n+} ($n \geq 3$) to Mn^{2+}. No clear separation was observed between these two processes, indicating that Mn^{n+} reduction starts before reduction of Cu^{2+} is completed. The perovskite with 50% substitution ($x = 0.5$, Fig. 5e) was more profoundly reduced at 973 K (2 e^- per molecule) than a similar sample, $LaMn_{0.5}Cu_{0.5}O_{2.93}$, prepared by Gallagher *et al.* (*18*) and Vogel *et al.* (*6*) which reduced only to $LaMn_{0.5}Cu_{0.5}O_{2.26}$ (i.e., to Mn^{2+} and Cu^+) at this temperature.

These different results are presumably due to the different experimental conditions used (10% H_2 + 90% N_2 flow and 20 K min^{-1} in the latter case). The curve for the sample with a substitution $x = 0.8$ (Fig. 6b) presents a complex profile derived from reduction of the different phases present, viz., $LaMn_{0.2}Cu_{0.8}O_{3+\lambda}$, La_2CuO_4, and CuO. However, the fully substituted sample ($x = 1$, Fig. 6c) shows two clear reduction steps, the first below 500 K due to CuO reduction and the second above 600 K due to reduction of the more stable La_2CuO_4 mixed oxide. In this case, the total weight loss measured upon reduction was found to be approximately that expected for reduction of Cu^{2+} to Cu^0. The reduction process for this sample ($x = 1$) can then be formulated according to the equation

$$La_2CuO_4 + CuO + 2H_2 \rightarrow La_2O_3 + 2Cu + 2H_2O. \quad (2)$$

This is supported by the X-ray diffraction results for reduced samples (see below). In Table 3 it is seen that the temperature for reduction to 1 e^- per molecule decreases for increasing substitution (x), i.e., the first stage of reduction becomes easier for increasing copper content.

The oxygen content in those samples where a single perovskite phase is present ($x = 0.6$) was determined from the measured weight loss in the TPR diagrams. The formulas of the compounds so calculated are given in Table 3. The perovskites show

TABLE 3

Stoichiometry of $LaMn_{1-x}Cu_xO_{3+\lambda}$ Oxides as Determined by TPR and Temperature for Reduction to 1 e^- per Molecule

Formula	T (K)
$LaMnO_{3.24}$	913
$LaMn_{0.8}Cu_{0.2}O_{3.13}$	718
$LaMn_{0.6}Cu_{0.4}O_{3.14}$	588
$LaMn_{0.5}Cu_{0.5}O_{3.00}$	583
$LaMn_{0.4}Cu_{0.6}O_{2.93}$	538

oxidative nonstoichiometry for $x = 0.4$ and reductive nonstoichiometry for $x = 0.6$. Stoichiometry is reached for $x = 0.5$. The nonsubstituted sample contains 48% Mn^{4+} which increases to ca. 100% for $0.4 \lesssim x \lesssim 0.6$. The stability of Mn^{4+} in a perovskite lattice has been well established. Jonker and van Santen (*1*) and Chengxian *et al.* (*10*) have reported ca. 85% Mn^{4+} in $LaMn_{1-x}M_xO_{3+\lambda}$ (M = Sr, Ca) after full substitution of La^{3+} by Sr^{2+} and Ca^{2+}, respectively. This behavior contrasts with that observed for $La_{1-x}Sr_xCoO_3$ where a maximum of 45% Co^{4+} was obtained for $x = 0.5$ (*38*). Higher substitutions resulted in a decrease in the percentage of Co^{4+}. The above results show that upon substitution of Mn^{n+} ($n \gtrsim 3$) by an ion of lower oxidation state, the charge compensation is achieved by manganese oxidation and also by a decrease in the oxygen content of the perovskite with the eventual appearance of oxygen vacancies.

Nonstoichiometry (excess or defect oxygen) of the perovskite samples ($0 \lesssim x \lesssim 0.6$) is represented as a function of manganese substitution in Fig. 7. The straight line shows the expected loss of oxygen with increasing copper content. Since, in this case, introduction of the substituting cation (Cu^{2+}) has taken place in position B of the structure, the rate of oxygen loss for increasing values of x is, of course, higher than that observed when the cation of lower oxidation state is introduced in position A [cf. Fig. 7 in this work with Fig. 4 in Ref. (*10*)]. Note that the unsubstituted perovskite exhibits an oxidative nonstoichiometry ($\lambda = 0.24$, Table 3) which is higher than those reported previously for $LnMnO_{3+\lambda}$ (Ln, rare-earth element) oxides ($0.1 \lesssim \lambda \lesssim 0.17$) (*1–10, 18, 39, 40*). Also, the substituted perovskites $LaMn_{1-x}Cu_xO_{3+\lambda}$ present an oxygen content higher than those reported by Gallagher *et al.* (*18*) and Vogel *et al.* (*6*) for similar compounds. This must be due to the relatively low heating temperature for preparation used in this work (973 K) compared with the temperatures used by other authors (1073–1673 K) (*1–10, 18, 39, 40*). These findings are in agreement with results indicating that λ in $LaMnO_{3+\lambda}$ tends to increase with decreasing calcination temperature (*1, 3, 5*).

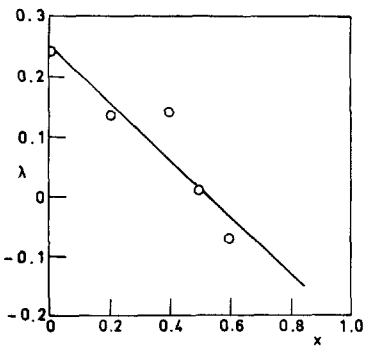

FIG. 7. Nonstoichiometry (λ) in $LaMn_{1-x}Cu_xO_{3+\lambda}$ as a function of copper content (x).

X-ray Diffraction of Reduced Samples

X-ray diffraction patterns were taken of reduced (after TPR experiments) samples. Selected diffractograms are shown in Fig. 8. The reduction products were La_2O_3, $La(OH)_3$, MnO, and Cu^0. MnO and Cu^0 diffraction lines decreased and increased, respectively, in intensity for increasing substitution of manganese. Note that the bulk La_2O_3 (*A* lines) is almost quantitatively converted to the hydroxide $La(OH)_3$ (*B* lines) after prolonged exposition to the atmosphere of the fully substituted sample ($x = 1$).

Particle sizes (d) were calculated by means of the Debye–Scherrer equation (*41*), $d = K\lambda/\beta \cos\theta$. K is a constant equal to 0.9; λ, the wavelength of the X-ray used; β, the broadening of the spectral line chosen, calculated by the expression $\beta^2 = B^2 - b^2$ (where B is the measured linewidth of Cu(111) or La_2O_3 (101) and b is the width measured under the same conditions with a substance of particles larger than 1000 Å); and θ, the diffraction angle of the line considered. These are given in Table 4. The particle size of La_2O_3 is practically constant regardless of the starting sample considered. However, d values for Cu^0 are strongly dependent on the copper content

of the sample. Thus, no Cu^0 lines were observed for low substitution of manganese by copper ($x < 0.5$), indicating that metallic copper is in a highly dispersed state on a matrix of La_2O_3 and MnO. For higher substitutions, particle sizes in the range $205 \leq d \leq 809$ Å were found. The large difference between d values for starting samples with $x = 0.8$ and $x = 1.0$ may be caused by the full conversion, in the latter case, of the perovskite into La_2CuO_4 and CuO (Fig. 1). Copper particle sizes for $0.5 \leq x \leq 1.0$ are remarkably larger than that found for Ni^0 (60 Å) produced by reduction of $LaNiO_3$ (*28*). In this last instance, reduction took place at 705 K, whereas in this work the final reduction temperature in the TPR experiments (Figs. 5 and 6) was 973 K. From our results, it can be concluded that the most favorable conditions for obtaining a highly dispersed copper catalyst are provided by reduction of a low-copper-content ($x < 0.5$) perovskite under isothermal conditions at 673 K or below (Fig. 4). High metal dispersions (beyond detection by X-ray diffraction) have been reported previously by Crespin and Hall (*42*) and Reller *et al.* (*43*) after reduction or oxidation–reduction cycles under controlled conditions of $LaCoO_3$ and $CaRuO_3$.

TABLE 4

Particle Sizes (d), as Determined by X-ray Line Broadening,[a] of Cu^0 and La_2O_3 Produced after Reduction in TPR Experiments of Samples with Nominal Composition $LaMn_{1-x}Cu_xO_{3+\lambda}$

Copper content (x)	d (Å)	
	Cu^0	La_2O_3
0	—	447
0.5	205	447
0.6	236	447
0.8	279	557
1.0	809	—

[a] Cu$K\alpha$ = 1.54 Å.

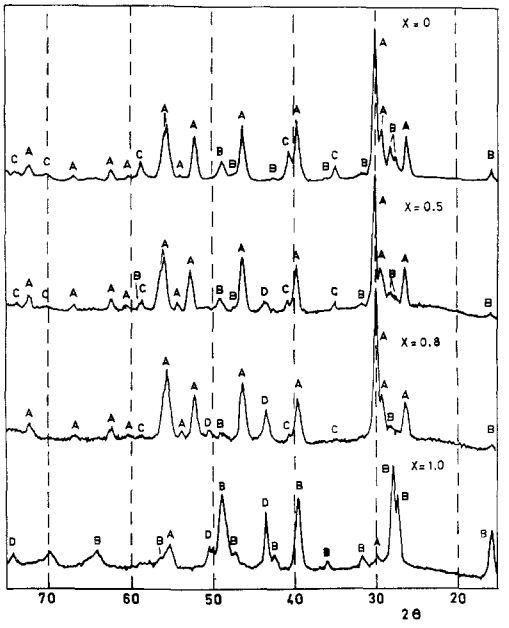

FIG. 8. X-ray diffraction patterns (Cu$K\alpha$ radiation) of samples with nominal composition $LaMn_{1-x}Cu_xO_{3+\lambda}$ after reduction in TPR experiments. (A) Hexagonal La_2O_3, (B) hexagonal $La(OH)_3$, (C) cubic MnO, (D) cubic Cu^0.

CONCLUSIONS

Substitution of manganese by copper in $LaMn_{1-x}Cu_xO_{3+\lambda}$ up to $x = 0.6$ preserves the perovskite structure. For $x = 0.8$, three phases, viz., $LaMn_{0.2}Cu_{0.8}O_{3+\lambda}$, La_2CuO_4, and CuO, were detected. For total manganese substitution ($x = 1$) the only phases present were La_2CuO_4 and CuO. $LaMnO_{3+\lambda}$ contains 48% Mn^{4+} which increases to ca. 100% for samples where $0.4 \leq x \leq 0.6$. The perovskites showed oxidative nonstoichiometry (excess oxygen) for $x \leq 0.4$ and reductive nostoichiometry (oxygen deficiency) for $x = 0.6$. $LaMn_{0.5}Cu_{0.5}O_3$ showed a stoichiometric composition ($\lambda = 0$). The charge compensation in $LaMn_{1-x}Cu_xO_{3+\lambda}$ oxides is achieved by manganese oxidation and by an oxygen loss with the eventual appearance of oxygen vacancies. The rate of this oxygen loss for increasing values of x when substitution of a cation B^{3+} by a cation of lower oxidation state takes place in position B of the structure is

higher than that recorded when the substitution takes place in position *A*. Comparison of our data with results reported in the literature supports the conclusion that λ in $LaMnO_{3+\lambda}$ tends to increase with decreasing calcination temperatures. Although the synthesis of $LaCuO_3$ has been reported in the literature, this perovskite appears not to be stable under our experimental conditions.

Samples with substitutions $0 \leq x \leq 0.6$ underwent reduction (in H_2) of Cu^{2+} to Cu^0 and reduction of Mn^{n+} ($n \geq 3$) to Mn^{2+}. In the fully substituted sample ($x = 1$) CuO reduced first and then La_2CuO_4. The temperature for reduction of the perovskites to 1 e^- per molecule decreased for increasing substitution (x); i.e., the first stage of reduction becomes easier for increasing copper content. Reduction of Mn^{3+} and Cu^{2+} in $LaMn_{1-x}Cu_xO_{3+\lambda}$ oxides is reached at substantially higher temperatures than reduction of manganese and copper in MnO_2 and CuO, showing the increased stability of transition metal cations in the perovskite structure.

The particle size (d) of La_2O_3 produced upon reduction of $LaMn_{1-x}Cu_xO_{3+\lambda}$ is practically constant regardless of the starting sample considered. However, d values for metallic copper are strongly dependent on the copper content of the sample. The most favorable conditions for obtaining a highly dispersed copper catalyst were found to be those attained by reduction of a perovskite with low copper content ($x < 0.5$) at 673 K or below.

ACKNOWLEDGMENT

This work has been sponsored by the Spanish–North American Joint Committee for Scientific and Technological Cooperation (Project CCB-8409/003), and the authors gratefully acknowledge the financial support received.

REFERENCES

1. Jonker, G. H., and van Santen, J. H., *Physica* **16,** 337 (1950).
2. Tofield, B. C., and Scott, W. R., *J. Solid State Chem.* **10,** 183 (1974).
3. Vrieland, E. G., *J. Catal.* **32,** 415 (1974).
4. Voorhoeve, R. J. H., Remeika, J. P., Trimble, L. E., Cooper, A. S., Disalvo, F. J., and Gallagher, P. K., *J. Solid State Chem.* **14,** 395 (1975).
5. Voorhoeve, R. J. H., Remeika, J. P., and Trimble, L. E., *Ann. N. Y. Acad. Sci.* **272,** 3 (1976).
6. Vogel, E. M., Johnson, D. W., Jr., and Gallagher, P. K., *J. Amer. Ceram. Soc.* **60,** 31 (1977).
7. Kamata, K., Nakajima, T., Hayashi, T., and Nakamura, T., *Mater. Res. Bull.* **13,** 49 (1978).
8. Nakamura, T., Petzow, G., and Gauckler, L. J., *Mater. Res. Bull.* **14,** 649 (1979).
9. Kamegashira, N., Miyazaki, Y., and Yamamoto, H., *Mater. Chem. Phys.* **11,** 187 (1984).
10. Chengxian, W., Bosheng, D., Shurong, F., Zuolong, Y., Xiaofan, X., and Yue, W., *Sci. Sin. B.* **27,** 778 (1984).
11. Misono, M., and Nitadori, T., *in* "Adsorption and Catalysis on Oxide Surfaces" (M. Che and G. C. Bond, Eds.), p. 409. Elsevier, Amsterdam, 1985.
12. Voorhoeve, R. J. H. *in* "Advanced Materials in Catalysis" (J. J. Burton and R. L. Garten, Eds.), p. 129. Academic Press, New York, 1977.
13. Watson, P. R., and Somorjai, G. A., *J. Catal.* **74,** 282 (1982).
14. Somorjai, G. A., and Davis, S. M., *Chemtech* **13,** 502 (1983).
15. Monnier, J. R., and Apai, G., *Amer. Chem. Soc. Div. Fuel Chem. Prepr. Pap.* **31**(2), 239 (1986).
16. Broussard, J. A., and Wade, L. E., *Amer. Chem. Soc. Div. Fuel Chem. Prepr. Pap.* **31**(3), 75 (1986).
17. Gysling, H. J., Monnier, J. R., and Apai, G., *J. Catal.* **103,** 407 (1987).
18. Gallagher, P. K., Johnson, D. W., Jr., and Vogel, E. M., *J. Amer. Ceram. Soc.* **60,** 28 (1977).
19. Gunsekaran, N., Meenakshisundaram, A., and Srinivasan, V., *Indian J. Chem.* **21A,** 346 (1982).
20. Tascón, J. M. D., Mendioroz, S., and Tejuca, L. G., *Z. Phys. Chem. N. F.* **124,** 109 (1981).
21. Demazeau, G., Parent, C., Pouchard, M., and Hagenmuller, P., *Mater. Res. Bull.* **7,** 913 (1972).
22. Happel, J., Hnatow, M., and Bajars, L., "Base Metal Oxide Catalysts," p. 117. Dekker, New York, 1977.
23. Khattak, C. P., and Wang, F. F. Y., "Handbook on the Physics and Chemistry of Rare Earths" (K. A. Gschneidner, Jr., and L. Eyring, Eds.), p. 525. North-Holland, Amsterdam, 1979.
24. Rao, C. N. R., Gopalakrishnan, J., and Vidyasagar, K., *Indian J. Chem.* **23A,** 265 (1984).
25. Vidyasagar, K., Reller, A., Gopalakrishnan J., and Rao, C. N. R., *J. Chem. Soc. Chem. Commun.,* 7 (1985).
26. Smyth, D. M., *Annu. Rev. Mater. Sci.* **15,** 329 (1985).
27. Crespin, M., Levitz, P., and Gatineau, L., *J. Chem. Soc. Faraday Trans. 2* **79,** 1181 (1983).

28. Fierro, J. L. G., Tascón, J. M. D., and Tejuca, L. G., *J. Catal.* **93,** 83 (1985).
29. Goodenough, J. B., and Longo, J. M., "Landolt–Börnstein New Series" (K. H. Hellwege and A. M. Hellwege, Eds.), Vol. 4, Part a, p. 126. Springer-Verlag, Berlin, 1970.
30. Wells, A. F., "Structural Inorganic Chemistry," 4th ed. p. 498. Oxford Univ. Press (Clarendon), London/New York, 1975.
31. Ichimura, K., Inoue, Y., and Yasumori., I., *Bull. Chem. Soc. Japan* **53,** 3044 (1980).
32. Yamazoe, N., Teraoka, Y., and Seiyama, T., *Chem. Lett.,* 1767 (1981).
33. Marcos, J. A., Buitrago, R. H., and Lombardo, E. A., *J. Catal.* **105,** 95 (1987).
34. Fierro, J. L. G., and Tejuca, L. G., *Appl. Surf. Sci.* **27,** 453 (1987).
35. Wachowski, L., Zielinski, S., and Burewicz, A., *Acta Chim. Acad. Sci. Hung. 106,* 217 (1981).
36. Fierro, J. L. G., Tascón, J. M. D., and Tejuca, L. G., *J. Catal.* **89,** 209 (1984).
37. Tascón, J. M. D., Fierro, J. L. G., and Tejuca, L. G., *J. Chem. Soc. Faraday Trans. 1* **81,** 2399 (1985).
38. Jonker, G. H., and van Santen J. H., *Physica* **19,** 120 (1953).
39. Yakel, H. L., *Acta Crystallogr.* **8,** 394 (1955).
40. Kamegashira, N., and Miyazaki, Y., *Mater. Res. Bull.* **19,** 1201 (1984).
41. Jelinek, Z. K., "Particle Size Analysis," Chap. 2, Series in Analytical Chemistry. Ellis Horwood, New York, 1974.
42. Crespin, M., and Hall, W. K., *J. Catal.* **69,** 359 (1981).
43. Reller, A., Davoodabady, G., Portmann, A., and Oswald, H. R., *in* "Proceedings, European Congress on Electron Microscopy, 8th, Budapest," p. 1165 (1984).